STUDY OF HIGGS PRODUCTION IN THE BOSONIC DECAY CHANNELS AT ATLAS

E. MOUNTRICHA
On behalf of the ATLAS Collaboration
Brookhaven National Laboratory, Department of Physics,
Upton, NY, United States

The latest results on the studies of the Higgs production in the bosonic decay channels at ATLAS are reported, involving the $H \to \gamma\gamma$, $H \to ZZ^{(*)}$, $H \to WW^{(*)}$ and $H \to Z\gamma$ decay channels. The full 2011 and 2012 LHC data samples have been used corresponding to 4.6-4.8 fb^{-1} at $\sqrt{s} = 7\,\text{TeV}$ and 20.7 fb^{-1} at $\sqrt{s} = 8\,\text{TeV}$, respectively.

1 Introduction

In summer 2012 the ATLAS and CMS collaborations announced the discovery of a Higgs-like boson [1,2]. Since then, the LHC Run I has been completed and the full data samples have been analyzed. The new particle's properties (mass, spin/parity, couplings) have been studied. In the following, the updated results on the signal strength and mass are presented, complemented with the studies on the properties of the new particle.

2 Updated results in the $H \to \gamma\gamma$ channel and properties measurement

$H \to \gamma\gamma$ is a high mass resolution channel with the simple topology of two high E_{T} isolated photons. The signal-background discriminating variable is the di-photon invariant mass, $m_{\gamma\gamma}$, (Figure 1 (left)) with an expected resolution of 1.77 GeV [3]. The signal-over-background (S/B) ratio is ∼3% in the mass region around $m_H = 125\,\text{GeV}$ containing 90% of the expected signal. The background processes are the irreducible di-photon continuum and events with jets misidentified as photons. To increase the sensitivity due to the different mass resolution and S/B ratio, and to separate the different production modes (gluon fusion (ggF), vector boson fusion (VBF) and associated production (VH)), 14 categories are used [3]. The excess observed at ∼126.5 GeV is quantified by the p_0 probability (Figure 1 (center)). The observed significance is $7.4\,\sigma$, while the expected one is $4.1\,\sigma$.

In Figure 1 (right) the best fit value of m_H and signal strength (μ), defined as the ratio of the observed number of signal events to the expected one from the Standard Model (SM), are

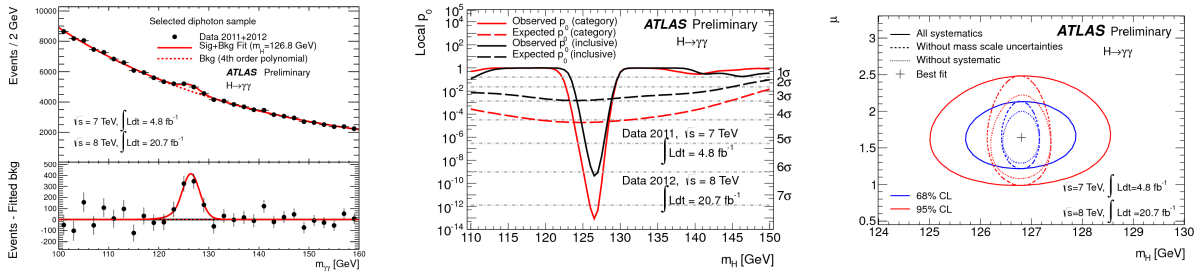

Figure 1: Left: Invariant mass distribution of di-photon candidates along with the signal-plus-background fit to the data. Center: The observed and expected local p_0 as a function of m_H. Right: The best-fit values of m_H and μ, and their 68% (blue) and 95% (red) CL contours. Ref. [3]

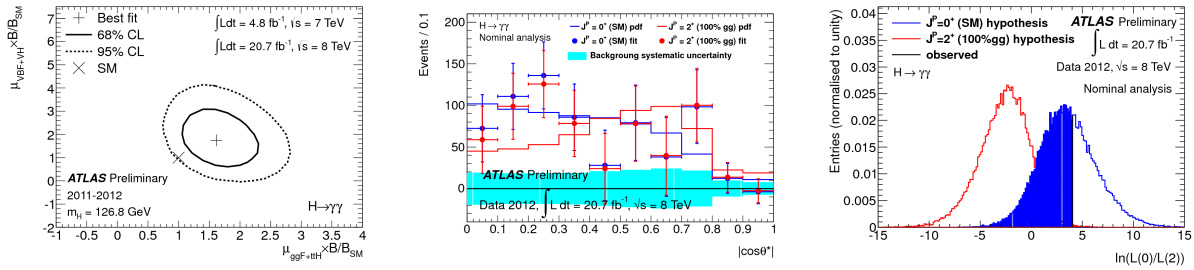

Figure 2: Left: The best-fit values of $\mu_{\mathrm{ggF+t\bar{t}H}}$ x $\mathrm{B/B_{SM}}$ and $\mu_{\mathrm{VBF+VH}}$ x $\mathrm{B/B_{SM}}$ and their 68% (solid) and 95% (dashed) CL contours. Center: Distribution of the background-subtracted data in the signal region as a function of $|\cos\theta^*|$. Right: Expected distributions of the test statistics q for the spin-0 and spin-2 hypotheses. Ref. [3,4]

shown. The mass is measured to be 126.8 ± 0.2 (stat) ± 0.7 (syst) GeV, where the systematic uncertainty is dominated by the photon energy scale uncertainties. The measured μ is 1.65 ± 0.24 (stat) $^{+0.25}_{-0.18}$ (syst). In the VBF enriched category a $2.0\,\sigma$ excess is observed at $m_H = 126.5$ GeV. The best fit signal strength grouped into the "bosonic" (VBF, VH) and "fermionic" (ggF, $\mathrm{t\bar{t}H}$) production modes is in agreement with the SM expectation within $2\,\sigma$ (Figure 2 (left)).

The new particle's spin has been studied comparing the SM spin-0^+ hypothesis to spin-2^+_m "graviton-like" with minimal couplings [4]. The discriminants used are the $m_{\gamma\gamma}$ and the angular distribution of the photons in the resonance rest frame, $|\cos\theta^*|$, (Figure 2 (center)). The observation is compatible with the spin-0^+ hypothesis and spin-2^+_m is excluded at 99.3% $\mathrm{CL_s}$ assuming the spin-2^+_m resonance is produced purely via gluon fusion (Figure 2 (right)).

3 Updated results in the $H \to ZZ^{(*)} \to 4\ell$ channel and properties measurement

$H \to ZZ^{(*)} \to 4\ell$, with $\ell = e, \mu$, is a high mass resolution channel with the very clean signature of two pairs of same-flavor, opposite-charge leptons. The four-lepton invariant mass ($m_{4\ell}$)

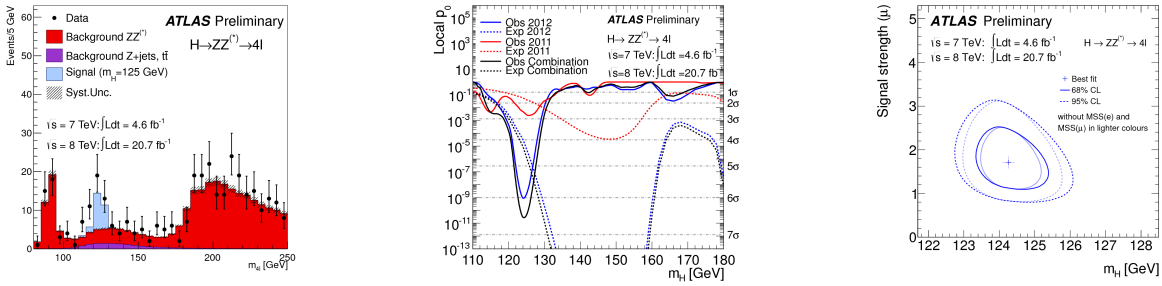

Figure 3: Left: The distribution of the four-lepton invariant mass, $m_{4\ell}$, for the selected candidates. Center: The observed and expected local p_0-value for the 2011 and 2012 data sets, and their combination. Right: Likelihood ratio contours in the μ-m_H plane that, in the asymptotic limit, correspond to 68% and 95% level contours. Ref. [5]

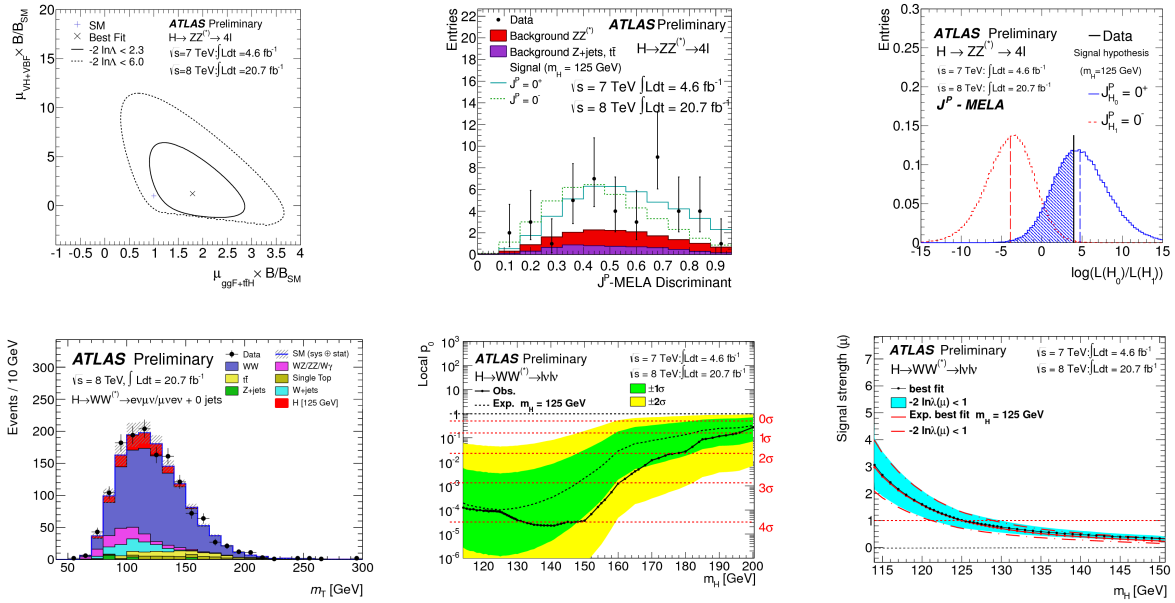

Figure 4: Left: Distribution of the transverse mass, m_{T}, for 8 TeV data for the $e\mu + \mu e$ channel in $\mathrm{N_{jet}} = 0$. Center: The observed and expected local p_0-value. Right: Signal strength as a function of m_H. Ref. [6]

discriminant (Figure 3 (left)) provides an expected resolution of 1.9 GeV with a S/B ratio of 1.6 at $m_H = 125\,\mathrm{GeV}$ [5]. The background processes consist of the irreducible $ZZ^{(*)}$ production and the reducible $t\bar{t}$ and Z+jets production estimated from control regions in data. To increase the sensitivity, categories are used according to the lepton flavor. The excess observed at 124.3 GeV (Figure 3 (center)) has a significance of $6.6\,\sigma$, while $4.4\,\sigma$ is expected.

The best fit value of m_H is $124.3^{+0.6}_{-0.5}$ (stat) $^{+0.5}_{-0.3}$ (syst) GeV, where the systematic uncertainty is dominated by the energy and momentum scale uncertainties while μ is $1.7^{+0.5}_{-0.4}$ (Figure 3 (right)). VBF and VH enriched categories have been added. The rates of various production modes are in agreement with the SM expectation within $2\,\sigma$ (Figure 3 (left)).

The spin of the new particle has been studied comparing the SM spin-0^+ to other spin/parity hypotheses. The discriminant ($\mathrm{J^P}$-MELA) for this study is based on five production and decay angles [5], and the dilepton invariant masses (m_{12}, m_{34}) (Figure 3 (center)). The observation is compatible with the SM spin-0^+ hypothesis while spin-0^- and spin-1^+ states are excluded at 97.8% $\mathrm{CL_s}$ or higher in favour of spin-0^+ (Figure 3 (right)).

4 Updated results in the $H \to WW^{(*)} \to \ell\nu\ell\nu$ channel and properties measurement

$H \to WW^{(*)} \to \ell\nu\ell\nu$ is a high rate but low mass resolution channel with the signature of two opposite charged isolated leptons and missing transverse energy ($E_{\mathrm{T}}^{\mathrm{miss}}$). Due to the presence of two neutrinos in the final state, a transverse mass is used as discriminant (m_{T}) (Figure 4 (left)). The S/B ratio ranges from 0.15-0.26 [6]. The background processes are $WW^{(*)}$, top, W+jets, Drell-Yan and diboson production, estimated from control regions in data. Categories are used based on the number of jets in the event and on the lepton flavor.

The significance of the observed excess at $m_H = 125\,\mathrm{GeV}$ is $3.8\,\sigma$, while $3.7\,\sigma$ is expected (Figure 4 (center)). At 125 GeV μ is 1.01 ± 0.21 (stat) ± 0.19 (theory) ± 0.12 (syst) ± 0.04 (lumi) (Figure 4 (right)), where the experimental systematic uncertainty is dominated by b-tagging efficiency and jet energy scale/resolution. The inclusive cross section has been calculated for $\sqrt{s} = 8\,\mathrm{TeV}$ and $m_H = 125\,\mathrm{GeV}$ to be $\sigma\cdot\mathrm{BR} = 6.0 \pm 1.1$ (stat) ± 0.8 (theory) ± 0.7 (syst) ± 0.3 (lumi) pb. An excess over background of $2.5\,\sigma$ is observed in the VBF enriched category assuming $m_H = 125\,\mathrm{GeV}$. The rates of the different production modes are in agreement with the SM expectation within $1\,\sigma$ (Figure 5 (left)).

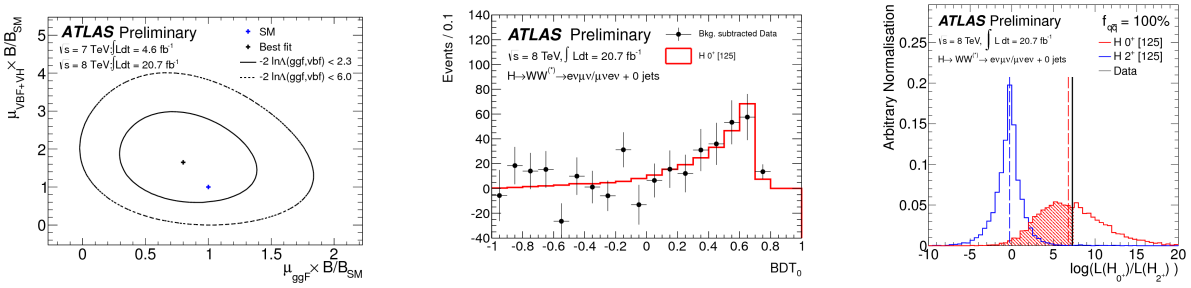

Figure 5: Left: Likelihood contours for separate ggF and VBF signal strength parameters. Center: The distribution for the spin analysis discriminant for spin-0^+ hypothesis. Right: Test statistics distributions when assuming the spin-0^+ hypothesis and testing the spin-2^+_m hypothesis. Ref. [6,8]

The new particle's spin has been studied using the 8 TeV data sample by comparing the SM spin-0^+ hypothesis to the spin-2^+_m. The discriminants (BDT [7]) for this study are based on $m_{\ell\ell}$, $m^{\mathrm{T}}_{\ell\ell}$, $\Delta\phi_{\ell\ell}$ and m_{T} (Figure 5 (center)) [8]. The observation is compatible with the SM spin-0^+ hypothesis while spin-2^+_m is excluded at more than 95% $\mathrm{CL_s}$ (Figure 5 (right)).

5 First results on the $H \to Z\gamma$ channel

$H \to Z\gamma$ is a high resolution but low rate channel with two opposite charged, isolated leptons and an isolated photon in the final state. The discriminant used in this channel is the $\Delta m = m_{\ell\ell\gamma} - m_{\ell\ell}$ and the mass resolution is $\sim$1.6 GeV. The background processes considered are the irreducible $Z\gamma$ production and events with Z and a jet misidentified as a photon. No excess has been observed in data. The observed upper limit on the SM Higgs production cross section for $m_H = 125$ GeV is $18.2\,\sigma_{\mathrm{SM}}$, while $13.5\,\sigma_{\mathrm{SM}}$ is the expected.

6 Summary

The first and preliminary results on the $H \to \gamma\gamma$, $H \to ZZ^{(*)} \to 4\ell$, $H \to WW^{(*)} \to \ell\nu\ell\nu$ and $H \to Z\gamma$ channels have been presented using the full LHC Run I ATLAS data. The signal significance in the individual $H \to \gamma\gamma$ and $H \to 4\ell$ channels is $\sim 7\,\sigma$. The signal strength and rates of the different production modes are found to be consistent with the SM expectation within 2σ, while observation is compatible with the spin-0^+ hypothesis.

References

1. ATLAS collaboration, *Phys. Lett.* B **716**, 1 (2012).
2. CMS collaboration, *Phys. Lett.* B **716**, 30 (2012).
3. ATLAS collaboration, ATLAS-CONF-2013-012, http://cdsweb.cern.ch/record/1523698.
4. ATLAS collaboration, ATLAS-CONF-2013-029, http://cdsweb.cern.ch/record/1527124.
5. ATLAS collaboration, ATLAS-CONF-2013-013, http://cdsweb.cern.ch/record/1523699.
6. ATLAS collaboration, ATLAS-CONF-2013-030, http://cdsweb.cern.ch/record/1527126.
7. B. P Roe *et al*, *Nucl. Instrum. Methods* A **543**, 577 (2005).
8. ATLAS collaboration, ATLAS-CONF-2013-031, http://cdsweb.cern.ch/record/1527127.
9. ATLAS collaboration, ATLAS-CONF-2013-009, http://cdsweb.cern.ch/record/1523683.